Cell Death and Differentiation (2007) 14, 306–317

www.nature.com/cdd

Eriocalyxin B induces apoptosis of t(8;21) leukemia cells through NF-κB and MAPK signaling pathways and triggers degradation of AML1-ETO oncoprotein in a caspase-3-dependent manner

L Wang[1,3], W-L Zhao[1,3], J-S Yan[1,3], P Liu[1,3], H-P Sun[1], G-B Zhou[1], Z-Y Weng[2], W-L Wu[1], X-Q Weng[1], X-J Sun[1], Z Chen*[,1], H-D Sun*[,2] and S-J Chen*[,1]

Diterpenoids isolated from Labiatae family herbs have strong antitumor activities with low toxicity. In this study, Eriocalyxin B (EriB), a diterpenoid extracted from *Isodon eriocalyx*, was tested on human leukemia/lymphoma cells and murine leukemia models. Acute myeloid leukemia cell line Kasumi-1 was most sensitive to EriB. Significant apoptosis was observed, concomitant with Bcl-2/Bcl-X_L downregulation, mitochondrial instability and caspase-3 activation. AML1-ETO oncoprotein was degraded in parallel to caspase-3 activation. EriB-mediated apoptosis was associated with NF-κB inactivation by preventing NF-κB nuclear translocation and inducing IκBα cleavage, and disturbance of MAPK pathway by downregulating ERK1/2 phosphorylation and activating AP-1. Without affecting normal hematopoietic progenitor cells proliferation, EriB was effective on primary t(8;21) leukemia blasts and caused AML1-ETO degradation. In murine t(8;21) leukemia models, EriB remarkably prolonged the survival time or decreased the xenograft tumor size. Together, EriB might be a potential treatment for t(8;21) leukemia by targeting AML1-ETO oncoprotein and activating apoptosis pathways.
Cell Death and Differentiation (2007) **14,** 306–317. doi:10.1038/sj.cdd.4401996; published online 16 June 2006

Acute myeloid leukemia (AML) is a group of hematopoietic malignancies arising from the abnormalities of proliferation, differentiation or survival of myeloid progenitors.[1] Specific chromosome translocations are frequently present in AML and play an important role in leukemia development.[2] The t(8;21)(q22;q22), representing the most common chromosome translocation in AML, generates the fusion oncoprotein AML1-ETO that is involved in leukemogenesis by blocking myeloid cells differentiation and apoptosis.[3] Clinically, although there is a high complete remission rate among t(8;21) AML patients using current chemotherapy protocol according to the reports from Western countries, a recent study in China showed that the 3-year disease-free survival was only 11%.[4] Moreover, high-dose chemotherapy is not suitable to elder patients.[5] Thus, development of an alternative therapy directly targeting the genetic aberrations of leukemia cells has become a priority.

Natural products have shown promising results in cancer therapy for the past 30 years.[6] These products provide many lead structures, which are subsequently used as templates for the design of novel compounds with enhanced biological properties. Paclitaxel, a natural product obtained from the bark of the Pacific yew *Taxus brevifolia*, shows efficacy against refractory breast and ovarian cancers, and hundreds of semisynthetic analogues have been produced, with more potential ones successfully applied in clinical trials.[6] In hematological diseases, inorganic arsenic compounds such as arsenic trioxide are greatly effective in the treatment of patients with acute promyelocytic leukemia.[7]

Oridonin is a diterpene compound isolated from the Chinese medicinal herb *Isodon rubescens*, and possesses significant antitumor activities in cancer cells. Eriocalyxin B (Figure 1a), an analogue of oridonin, is a natural ent-kaurene diterpene compound purified from *Isodon eriocalyx* var. *laxiflora*, a perennial herb of the Labiatae family distributed in the south-west China and used as an anti-inflammatory and antibacterial agent in local folk medicine.[8] EriB was tested for their cytotoxicity on human tumor cells and showed significant inhibitory effects on HL60, A549, MKN-28, HCT and CA cells. It has been proposed that the active sulfhydryl (SH) groups of

[1]State Key Laboratory of Medical Genomics, Shanghai Institute of Hematology, Rui Jin Hospital, Institute of Health Science, Shanghai Institutes for Biological Sciences and Graduate School, Chinese Academy of Sciences and School of Medicine, Shanghai Jiao Tong University, Shanghai 200025, China and [2]Kunming Institute of Botany, Chinese Academy of Sciences, Kunming 650204, Yunnan, China

*Corresponding authors: S-J Chen, State Key Laboratory of Medical Genomics, Shanghai Institute of Hematology, Rui Jin Hospital, School of Medicine, Shanghai Jiao Tong University, 197 Rui Jin Er Road, Shanghai 200025, China. Tel: +86 21 64377859; Fax: +86 21 64743206; E-mail: sjchen@stn.sh.cn or Z Chen, E-mail: zchen@stn.sh.cn and H-D Sun, Kunming Institute of Botany, Chinese Academy of Sciences, Kunming 650204, Yunnan, China. E-mail: hdsun@mail.kib.ac.cn

[3]These authors equally contributed to this work

Keywords: eriocalyxin B; acute myeloid leukemia; apoptosis; NF-κB; MAPK; AML1-ETO

Abbreviations: EriB, eriocalyxin B; AML, acute myeloid leukemia; SH, sulfhydryl; IC_{50}, fifty percents of growth inhibition concentration; $\Delta\psi_m$, mitochondrial membrane potential; p-ERK1/2, phosphorylated form of ERK1/2; MTT, 3-(4,5-dimethylthiazol-2-yl)-2,5-diphenyltetrazolium bromide; PI, propidium iodide; Rh123, rhodamine 123; DCFH-DA, dichlorofluorescein diacetate; TNF-α, tumor necrosis factor alpha; DTT, dithiothreitol; PARP, poly (ADP-ribose) polymerase; ROS, reactive oxygen species; GSH, glutathione; OS, overall survival; NP-40, Nonidet P-40; HEPES, N-2-hydroxyethylpiperazine-N′-2-ethanesulfonic acid; RT-PCR, reverse transcription PCR; OD, optical density

Received 25.11.05; revised 02.5.06; accepted 16.5.06; Edited by R De Maria; published online 16.6.06

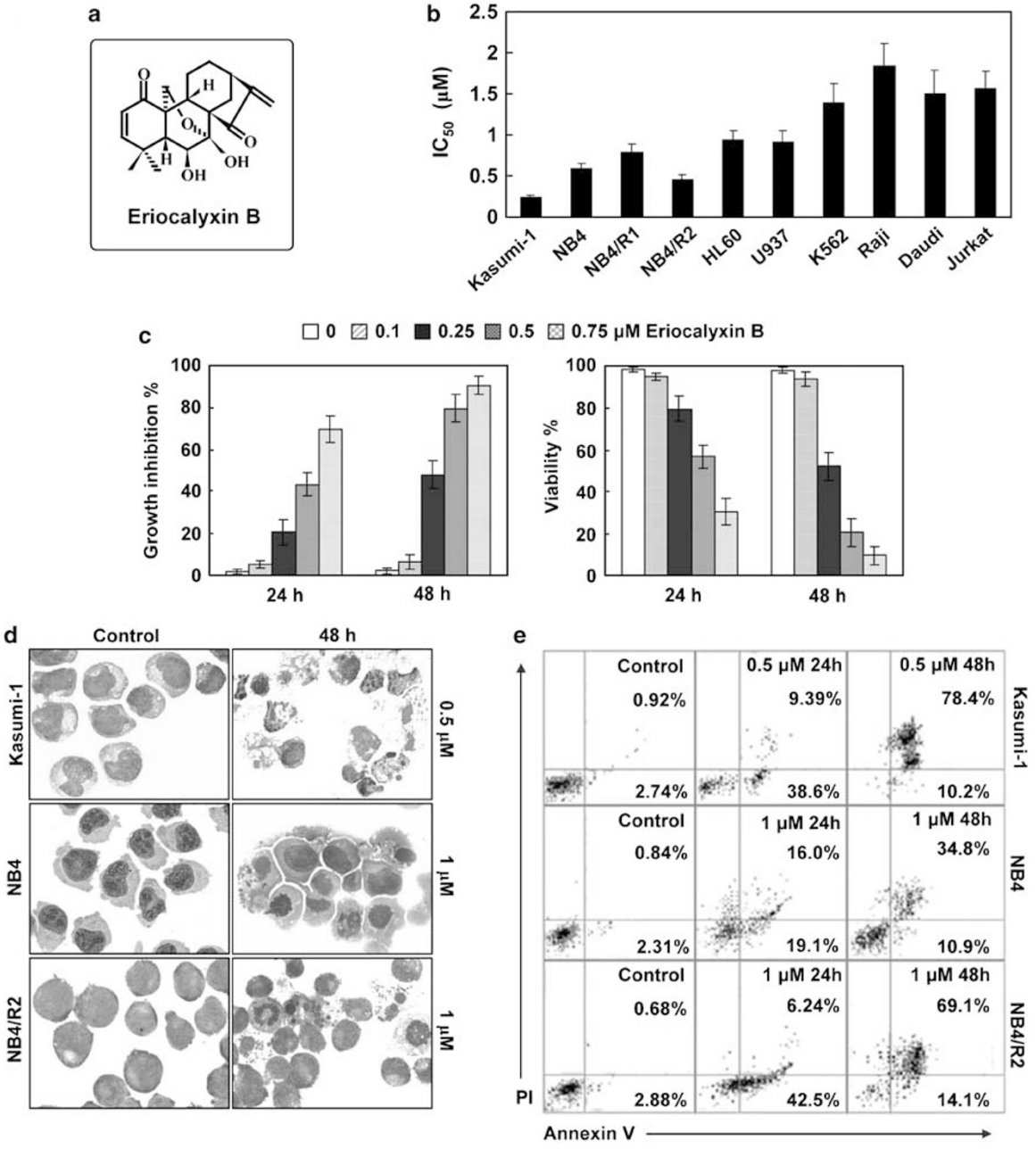

Figure 1 The effect of EriB treatment on growth and apoptosis of human leukemia and lymphoma cell lines. (**a**) Chemical structure of EriB (adapted from H-D Sun). (**b**) IC_{50} results obtained from MTT assay in leukemia and lymphoma cell lines treated with EriB. The IC_{50} values of Kasumi-1, NB4, NB4/R1 and NB4/R2 were below 1 μM. (**c**) The growth inhibition and cell viability of Kasumi-1 cells treated with EriB for 24 and 48 h at the indicated concentrations. Significant inhibitory effects with reduced cell viability were detected in Kasumi-1 cells from 0.25 μM EriB. Each column represented the mean $\pm$ S.D. in triplicates in three independent experiments. (**d**) Characteristic apoptotic cells were presented in Kasumi-1, NB4 and NB4/R2 cells treated with 0.5 or 1 μM EriB for 48 h. (**e**) Annexin V analysis of Kasumi-1, NB4 and NB4/R2 cells treated with EriB for 24 and 48 h. EriB treatment increased the percentages of annexin-V^+/PI^- (down right quadrant) and annexin-V^+/PI^+ (up right quadrant) cells

biological molecules could be the target of EriB, although the precise mechanism of action remains to be investigated.[9]

In the present study, we first assessed the effect of EriB on a series of hematopoietic malignant cell lines. The results indicated that EriB induced preferentially apoptosis of t(8;21) leukemia cells. It not only downregulated Bcl-2 and Bcl-X_L expression, resulting in mitochondrial instability and caspase-3 activation, but also targeted AML1-ETO oncoprotein in a caspase-3-dependent manner. A multiple mechanism was involved in EriB-mediated apoptosis, including inhibition of NF-κB activity and dysregulation of MAPK-signaling pathway. Thereafter, using murine t(8;21) leukemia models, we further proved that EriB significantly prolonged the survival time or reduced xenograft tumor size. All these preclinical studies suggested that EriB may have potentials in the treatment of t(8;21) leukemia.

Results

EriB inhibited cell growth and induced cell apoptosis in human leukemia cell lines. Using MTT assay, we determined the effect of EriB on human hematopoietic malignant cell lines. Fifty percents of growth inhibition (IC_{50}) was measured in these cells treated with EriB at concentrations ranging from 0.2 to 2 μM. EriB exerted substantial growth inhibition in myeloid cell lines examined. The IC_{50} values showed 0.2 μM in Kasumi-1 cells, about 0.5 μM in NB4 and NB4/R2 cells, and approximately 1 μM in NB4/R1, HL60 and U937 cells. The sensitivity of malignant lymphoid cell lines to EriB was lower than those of myeloid leukemia cells, with IC_{50} higher than 1.5 μM in Raji, Daudi and Jurkat cells (Figure 1b).

Kasumi-1 cells were most sensitive to EriB and cell growth was inhibited in a time- and dose-dependent manner, corresponding to the reduced cell viability (Figure 1c). This cell death inducing effect was observed at the concentration 0.25, 0.5 and 0.75 μM. At 48 h of treatment, 0.25 μM EriB produced 42.7 $\pm$ 6.5% cell death and 0.75 μM EriB resulted in 90.5 $\pm$ 4.3% cells death (Figure 1c, left panel).

To confirm whether the growth inhibition of EriB was caused by apoptosis, cell morphology and annexin V-FITC/PI double staining were analyzed. Kasumi-1 cells treated with 0.5 μM EriB presented characteristic morphological changes of apoptosis, such as shrinking cytoplasm, condensed chromatin and nuclear fragmentation with intact cell membrane, which could also be observed in 1 μM EriB-treated NB4 and NB4/R2 cells (Figure 1d). The percentage of annexin V-positive cells increased to 88.6% in Kasumi-1 cells at 48 h of 0.5 μM EriB treatment, which was higher than those of 1 μM EriB-treated NB4 and NB4/R2 cells (Figure 1e).

Cell cycle of Kasumi-1 cells was examined in the presence of EriB at 0.25 μM for 6, 12, 24, 36 and 48 h. No significant changes of G1, S and G2/M proportions was observed in EriB-treated cells, compared with those from the control (56.2, 36.5 and 7.3%, respectively). Of note, the analysis of nuclear DNA distribution showed a time-dependent increase of sub-G_1 cells content, indicating EriB-induced apoptosis (Figure 2a).

Differentiation-related antigens of myelocyte and monocyte were also evaluated. There was no obvious change in the expression of CD11b, CD13, CD14, CD33, CD34 and CD64 in Kasumi-1 cells treated with 0.1 and 0.25 μM EriB for 7 days (data not shown).

EriB-induced apoptosis was associated with mitochondria damage and caspase-3 activation. To search for the indication of mechanisms involved in apoptosis, ultrastructure of Kasumi-1 cells was studied. Compared with irregularly shaped nuclei, abundant rough endoplasmic reticulum and mitochondria in control cells (Figure 2b, upper panel), Kasumi-1 cells treated with 0.5 μM EriB for 4 h revealed inflated cells, swelling and vacant mitochondria and increased numbers of lysosomes, indicating early cell apoptosis and the damage in mitochondria (Figure 2b, lower panel).

Marked dissipation of mitochondrial membrane potential ($\Delta\psi_m$), as shown by the decrease in Rh123 fluorescence,[10] was observed in Kasumi-1 cells treated with EriB in a dose- and time-dependent manner (Figure 2c). In parallel to $\Delta\psi_m$ loss, after 24 h of EriB treatment, caspase-3 was cleaved into its active form in Kasumi-1, NB4 and NB4/R2 cells (Figure 2d). PARP was cleaved to an 85-kDa fragment (ΔPARP) and further degraded by EriB treatment in Kasumi-1 cells (Figure 2d). These data suggested that EriB induced cell apoptosis through an intrinsic mitochondrial pathway depending upon caspase activation.

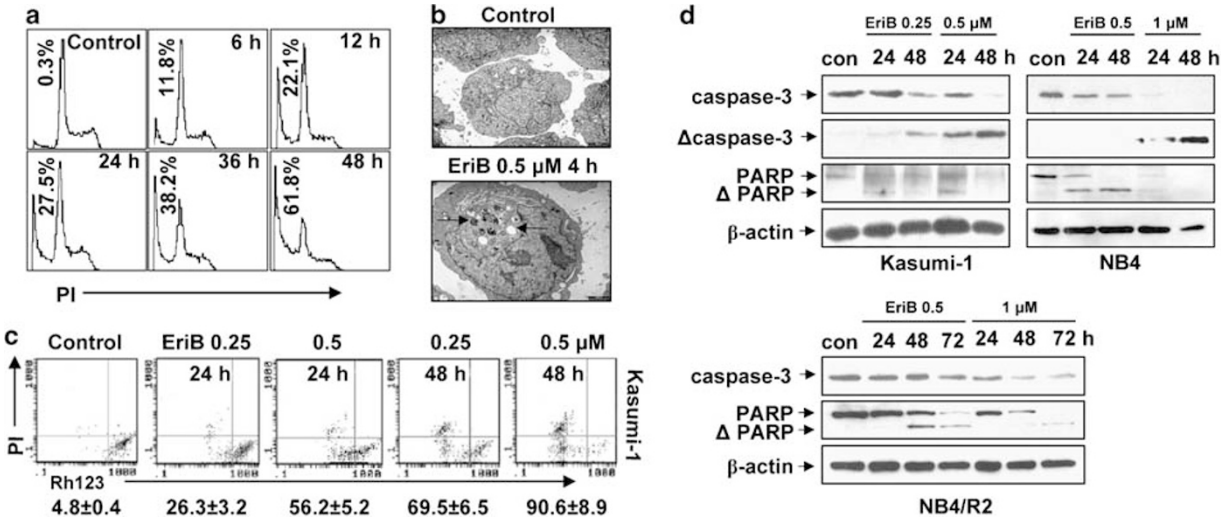

Figure 2 EriB induced the increase of sub-G_1 cells, mitochondrial transmembrane potential collapse and caspase-3 activation. (**a**) Contribution of nuclear DNA content in Kasumi-1 cells treated with 0.25 μM EriB for 6, 12, 24, 36 and 48 h. Significant increase of sub-G_1 cells was observed. (**b**) Ultrastructure of Kasumi-1 cells. Comparing with the control cells (upper panel, $\times$ 7400), EriB-treated Kasumi-1 cells (lower panel, $\times$ 7400) presented mitochondrial damage and increasing amount of lysosome (Arrows). (**c**) The mitochrondrial transmembrane potential was decreased in Kasumi-1 cells treated with EriB for 24 and 48 h. The numbers below the scatter plots represented the percentage of Rh123 low cells. (**d**) Western blot analysis of caspase-3, active (Δ) caspase-3 and PARP proteins with β-actin as a loading control. In Kasumi-1, NB4 and NB4/R2 cells treated with EriB, caspase-3 was activated with PARP cleaved

EriB acted on intrinsic apoptotic pathway through downregulation of Bcl-2 and Bcl-X_L. Mitochondrial membrane permeability is directly controlled by Bcl-2 family proteins, which are the central regulators of caspase activation.[11] To determine whether EriB damaged mitochondria through affecting these Bcl-2 family members, the expression of antiapoptotic factor Bcl-2 and Bcl-X_L, as well as proapoptotic factor Bax and Bcl-X_S were investigated in Kasumi-1 cells after 24 and 48 h of incubation with EriB. The Bcl-2 and Bcl-X_L expression were decreased at both protein and mRNA levels, whereas no significant changes of Bax and Bcl-X_S was detected (Figure 3a and b). Consequently, EriB induced negative modulation of Bcl-2/Bax and Bcl-X_L/Bax ratios (Figure 3c and d), which were consistent with the disturbed mitochondria stability and Kasumi-1 cells apoptosis. In Kasumi-1 cells transfected with expression vectors, and thereby with Bcl-2 or Bcl-X_L overexpression, EriB could only partially reduce Bcl-2 or

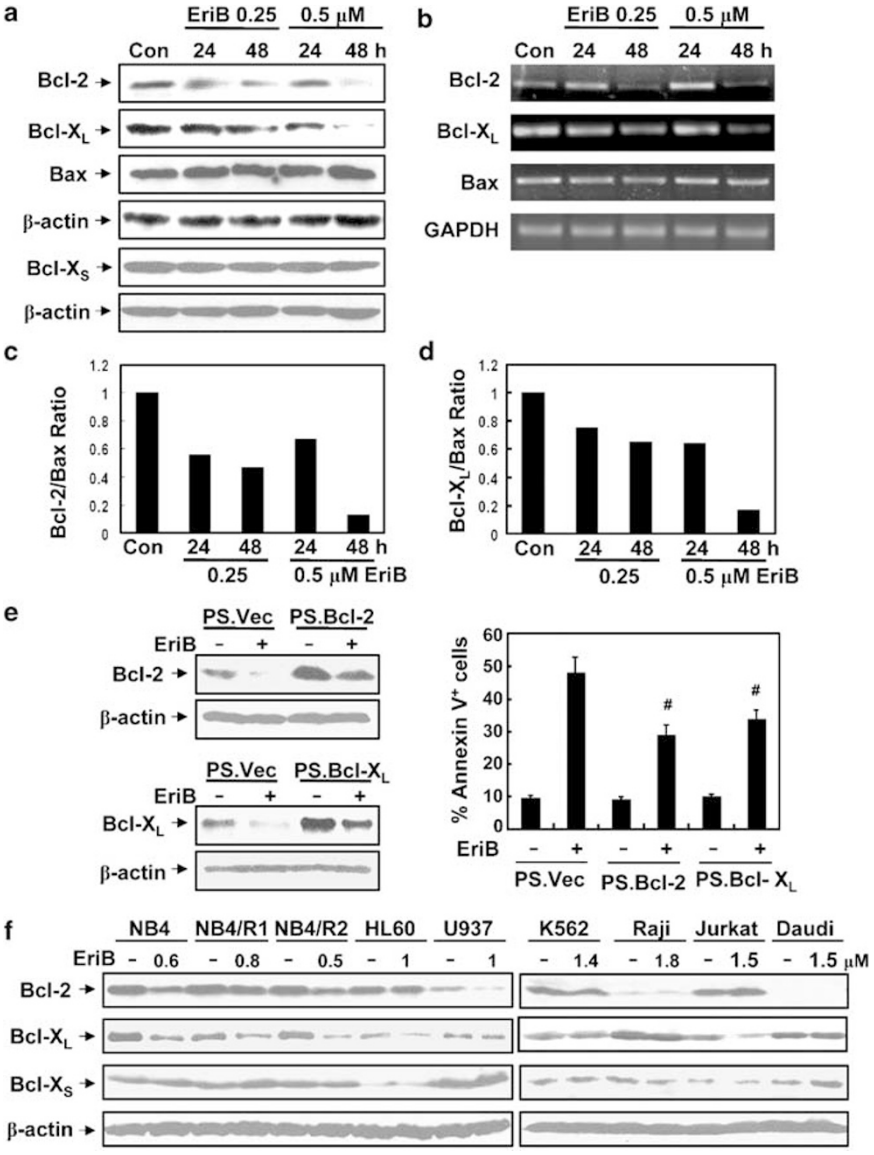

Figure 3 EriB decreased Bcl-2 and Bcl-X_L, but not Bcl-X_S and Bax, at protein and mRNA levels in Kasumi-1 cells. (**a** and **b**) The expression of Bcl-2, Bcl-X_L, Bax and Bcl-X_S protein were determined by Western blot (**a**), and their mRNA levels were detected using RT-PCR (**b**). Bcl-2 and Bcl-X_L, but not Bax, were reduced in both protein and mRNA levels in Kasumi-1 cells treated with 0.25 and 0.5 μM EriB for 24 and 48 h. (**c** and **d**) EriB induced the negative modulation of Bcl-2/Bax and Bcl-X_L/Bax ratios. The intensity of the bands was quantified by densitometry. The graphs represented the optical density (OD) of Bcl-2/Bax and Bcl-X_L/Bax ratio normalized to the OD of β-actin of a representative experiment for Western blot analysis. (**e**) Bcl-2- or Bcl-X_L-overexpressing Kasumi-1 cells were resistant to EriB-induced apoptosis. Kasumi-1 cells were transiently transfected with pSFFV/Bcl-2 (PS.Bcl-2), pSFFV/Bcl-X_L (PS.Bcl-X_L) or control plasmid pSSFV (PS.Vec). After 24 h of transfection, cells were exposed to EriB (0.5 μM) for 24 h. Bcl-2 and Bcl-X_L were detected by Western blot (left panel) and cell apoptosis was examined by Annexin V analysis (right panel). Each column represented the mean $\pm$ S.D. in triplicates in three independent experiments (#, $P<0.05$ *vs.* PS.Vec). (**f**) The expression of Bcl-2 or Bcl-X_L, but not Bcl-X_S, were differentially regulated according to their sensitivity to EriB. NB4, NB4/R1, NB4/R2, HL60, U937, K562, Raji, Jurkat and Daudi cells, were treated with or without EriB for 48 h at their own concentrations of IC_{50} (as shown in Figure 1b). The expression of Bcl-2, Bcl-X_L and Bcl-X_S protein were examined

Bcl-X_L expression and the EriB-induced apoptosis was partially attenuated (Figure 3e).

In other cells tested, Bcl-2 or Bcl-X_L expression were differentially regulated according to their sensitivity to EriB, while Bcl-Xs expression was not affected. Upon treatment with EriB, most obvious decrements of Bcl-2 protein level were found in NB4, NB4/R2 and U937 cells, and of Bcl-X_L protein level in NB4, NB4/R1, NB4/R2, HL60 and U937 cells. However, in those cells that were relatively insensitive to EriB, such as K562, Raji, Jurkat and Daudi cells, the levels of Bcl-2 or Bcl-X_L were less affected (Figure 3f).

EriB inhibited both intrinsic and TNF-α-induced NF-κB activation in Kasumi-1 cells. EriB decreased the mRNA levels of Bcl-2 and Bcl-X_L, which are known to be transcriptionally regulated by NF-κB.[12,13] To investigate whether EriB is capable of blocking intrinsic and TNF-α-mediated NF-κB activation, luciferase assays were performed. A basal transcriptional activity of NF-κB was observed, indicating that NF-κB is constitutively activated in Kasumi-1 cells. Luciferase activity was increased approximately fourfold by the addition of TNF-α for 4 h (Figure 4a). Pretreatment of cells with EriB for 1 h could block both intrinsic and TNF-α-mediated NF-κB activation (Figure 4a). However, EriB and TNF-α alone or combination had no effect on P65 protein levels (Figure 4a). EMSA assays showed that Kasumi-1 cells treated with TNF-α displayed remarkable upregulation of NF-κB activity, whereas EriB added 1 h prior to TNF-α treatment blocked the NF-κB activation (Figure 4b, middle panel). However, the inhibitory effect could be diminished by cotreatment with 0.2 mM DTT, a widely used disulfide-bond-reducing agent (Figure 4b, right panel), suggesting that the inhibitory effect was probably redox-sensitive. The specific NF-κB complex in Kasumi-1 cells was analyzed, and the protein-DNA complex corresponded to P65 (Figure 4b, left panel). These results suggested that NF-κB is constitutively activated in Kasumi-1 cells, while EriB is able to inhibit intrinsic and TNF-α-induced NF-κB activation.

EriB prevented NF-κB nuclear translocation and induced IκBα cleavage in Kasumi-1 cells. To further understand the mechanism of EriB-mediated NF-κB inactivation, we conducted immunofluorescence assay and Western blot analysis to examine the NF-κB (P65) nuclear translocation. Although EriB alone had no obvious effect on P65 nuclear translocation, it could significantly block the rapid nuclear translocation of P65 induced by TNF-α in Kasumi-1 cells (Figure 4c). Accordingly, the nuclear content of NF-κB was decreased with its accumulation in cytoplasm after EriB treatment (Figure 4d). To assess the effect of EriB on the nuclear NF-κB, nuclear protein extracts were prepared from Kasumi-1 cells. A decrease in P65 was seen in the nucleus of Kasumi-1 cells treated with EriB for 24 and 48 h (Figure 4e).

It has been shown that IκBα regulates NF-κB activation by sequestering it in the cytoplasm. Nuclear translocation of NF-κB occurs as a result of ubiquitination and subsequent proteasomal degradation of IκBα.[13] In our study, TNF-α addition induced IκBα phosphorylation/degradation within 4 h, while pretreatment with EriB inhibited these changes (Figure 4d). Interestingly, using anti-C-terminus IκBα antibody, but not anti-N-terminus IκBα antibody, we detected two protein species of 37 and 34 kDa (Figure 4e). These results suggested that EriB induced IκBα cleavage to a 34-kDa product (ΔIκBα), which may produce a super-repressive effect on NF-κB by stably sequestering it within the cytosol.[14]

Together, EriB could inhibit intrinsic NF-κB activation by directly restraining its DNA-binding activity and blocking TNF-α-induced NF-κB activation mainly via inhibiting phosphorylation and degradation of IκBα.

EriB changed ROS and GSH levels in Kasumi-1 cells. It was shown that diterpenoids exert their toxic effects by interacting with active SH groups. To understand whether this mechanism is involved in EriB-induced apoptosis, we treated Kasumi-1 cells simultaneously with 0.5 μM EriB and 0.2 mM DTT. Although DTT alone had no substantial effect on cell apoptosis, it completely blocked apoptosis induced by EriB (Figure 4f, left panel).

To investigate whether ROS level was also affected by EriB, we used flow cytometric analysis with a cell-permeable dye, H2DCFDA, which is specifically cleaved to emit a fluorescence wavelength in the presence of ROS. Treatment with 0.5 μM EriB alone for 2 h caused an approximately twofold elevation of ROS level in Kasumi-1 cells compared with untreated cells, whereas cotreatment with 0.2 mM DTT caused no significant changes (Figure 4f, middle panel). Meanwhile, GSH levels, as the main determinant of intracellular redox status, were significant depleted, after 2, 4 and 12 h of 0.5 μM EriB treatment (Figure 4f, right panel).

EriB induced caspase-3-dependent degradation of AML1-ETO oncoprotein. AML1-ETO, generated by the chromosomal translocation t(8;21), is an important therapy target in the treatment of AML containing the fusion protein.[15] Using anti-ETO antibody, we found that AML1-ETO was degraded in Kasumi-1 cells treated with EriB for 24 and 48 h and the degradation was consistent with caspase-3 activation (Figure 5a, left panel). Of note, other caspase-3 activators like arsenic trioxide (2 μM) and cytarabine (50 μM) were also able to induce Kasumi-1 cells apoptosis and cause AML1-ETO degradation, although to a less extent as compared to EriB treatment when the degree of caspase-3 activation was similar (Figure 5a, right panel).

To further verify the role of caspase-3 activation on AML1-ETO degradation and EriB-induced apoptosis, Kasumi-1 cells were treated with EriB in the presence or absence of the caspase-3 inhibitor Z-DEVD-fmk.[16] Z-DEVD-fmk (40 μM) could significantly block EriB-induced caspase-3 activation and PARP cleavage, resulting in persistence of AML1-ETO oncoprotein (Figure 5b). However, induction of Kasumi-1 cell apoptosis by 0.5 μM EriB was only partly attenuated by the addition of Z-DEVD-fmk 1 h before EriB treatment as manifested by the percentage of annexin V-positive cells (Figure 5c), suggesting that EriB-induced AML1-ETO degradation is an event accompanying caspase-3 activation, whereas there may exist caspase-3 independent mechanisms involved in EriB-induced apoptosis.

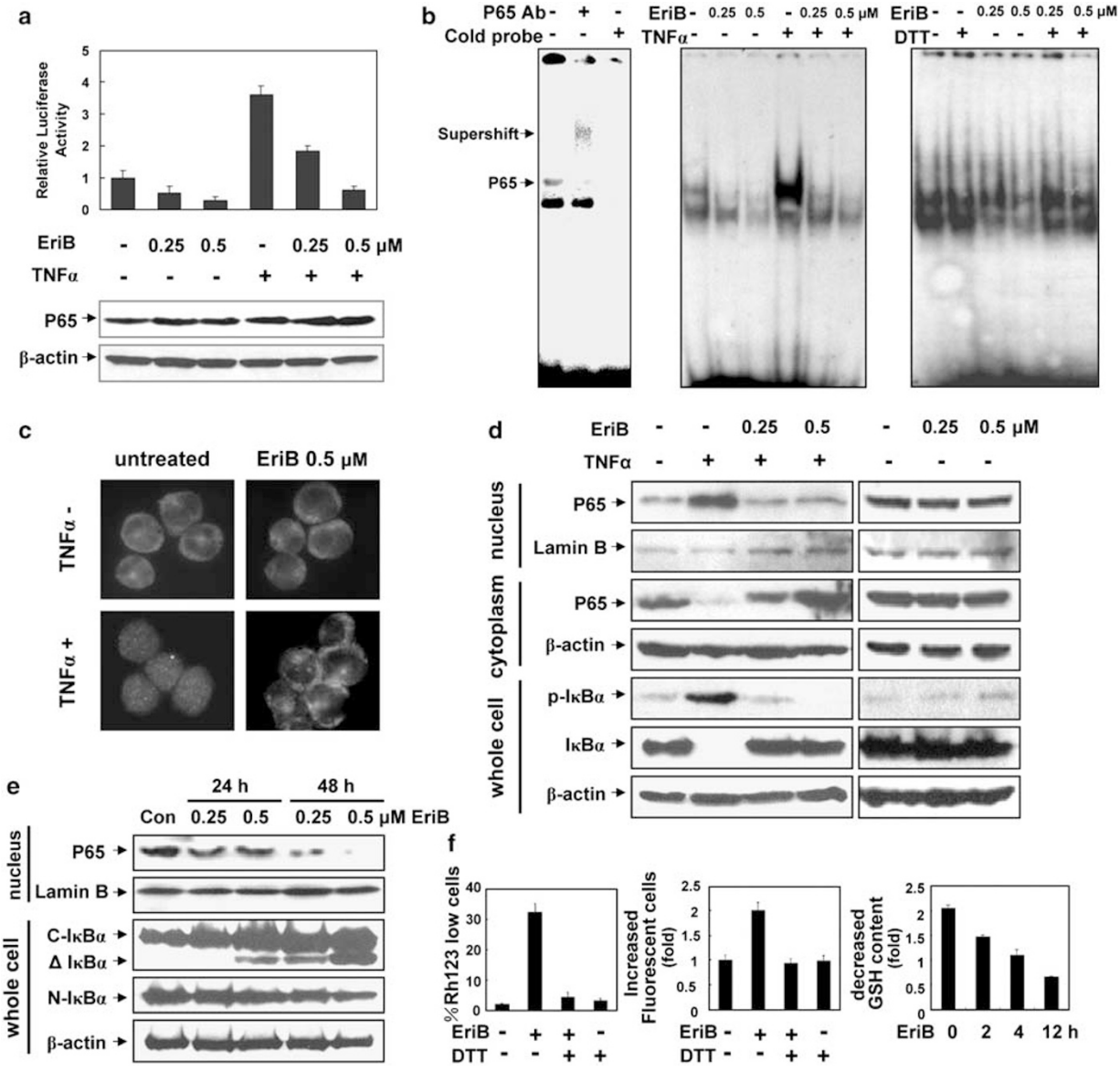

Figure 4 EriB inhibited intrinsic and TNFα-induced NF-κB activation in Kasumi-1 cells. (**a**) EriB downregulated NF-κB-dependent transcription in luciferase assay. Kasumi-1 cells were transiently transfected with an NF-κB-directed luciferase reporter plasmid and a β-gal plasmid. After pretreatment with 0.25 and 0.5 μM EriB for 1 h, TNF-α was added for 4 h. Each column represented the mean $\pm$ S.D. in triplicates in three independent experiments (upper panel). NF-κB (P65) was detected by Western blot (lower panel). (**b**) EriB inhibited the DNA-binding activity of NF-κB. NF-κB subunit specificity was determined by using anti-P65 antibody and cold probe (left panel), and arrow indicated the position of supershift band. Kasumi-1 cells were treated under the same condition as (**a**) (middle panel), and incubated with DTT (0.2 mM), EriB (0.25 and 0.5 μM) or EriB combined with DTT for 4 h, respectively (right panel). Nuclear extracts were prepared, and DNA-binding activity of NF-κB was studied by electrophoretic mobility shift assays. (**c**) The intracellular translocation of P65 was analyzed by immunofluorescence in Kasumi-1 cells. NF-κB (P65) was mainly located in cytoplasm in untreated cells and a significant P65 staining was found in the cell nucleus treated with 100 ng/ml TNF-α for 4 h. Pretreatment with 0.5 μM EriB for 1 h could block this translocation induced by TNF-α. (**d**) EriB induced IκBα phosphorylation and degradation in the presence of TNF-α. Kasumi-1 cells were incubated with EriB for 1 h prior to stimulation by 100 ng/ml TNF-α for 4 h. Nuclear and cytoplasmic proteins were prepared for Western blot to detect P65. Lamin B was used as a nuclear protein control. Equal proteins from whole cell lysates were also analyzed with antibodies specific for the phosphorylated form of IκBα (p-IκBα) and total IκBα. (**e**) EriB induced the decrease of P65 in nucleus and the cleavage of IκBα. Kasumi-1 cells were treated with 0.25 and 0.5 μM EriB for 24 and 48 h. Nuclear proteins were extracted and subjected to Western blot for P65 detection. IκBα proteins in whole cell lysates were determined with anticarboxyl-terminal IκBα (C-IκBα) and antiamino-terminal IκBα (N-IκBα) antibodies. Mobilities of IκBα and ΔIκBα are indicated with arrows. (**f**) DTT inhibited EriB-induced apoptosis as well as ROS generation, and EriB decreased the GSH content in Kasumi-1 cells. Cells were incubated with 0.2 mM DTT and 0.5 μM EriB for 12 h. The mitochrondrial transmembrane potential was measured on flow cytometry. *Left panel:* percentages of Rh123-low cells. Cells were treated with 0.2 mM DTT and 0.5 μM EriB for 2 h. *Middle panel:* the increased fold of fluorescent cells. Cells were treated with 0.5 μM EriB for 2, 4 and 12 h. *Right panel:* the decreased fold of GSH content. Each column represented the mean $\pm$ S.D. in triplicates in three independent experiments

EriB dysregulated MAPK signaling pathway in Kasumi-1 cells. The Ras/Raf/MEK/ERK pathway is an important signaling cascade involved in the control of hematopoietic cell proliferation and interruption of this pathway predominates proapoptotic signals in AML cells.[17] By Western blot, a rapid decrease of ERK1/2 phosphorylation was observed in

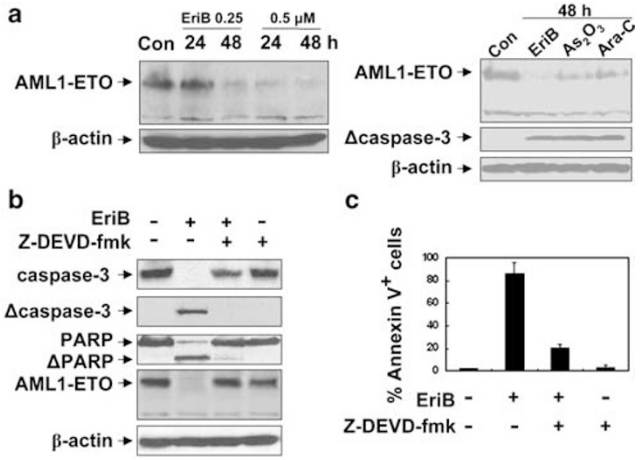

Figure 5 EriB induced the degradation of AML1-ETO oncoprotein, which could be completely inhibited by Z-DEVD-fmk. (**a**) EriB induced AML1-ETO degradation in Kasumi-1 cells. Kasumi-1 cells were treated with 0.25 and 0.5 μM EriB for 24 and 48 h. AML1-ETO protein in whole cell lysates was determined using anti-ETO antibody (left panel). Like EriB, other caspase-3 activators as arsenic trioxide (2 μM) and cytarabine (50 μM) also induced AML1-ETO protein degradation and caspase-3 activation at 48 h (right panel). (**b**) Western blot analysis of caspase-3, active (Δ) caspase-3, PARP and AML1-ETO proteins. Kasumi-1 cells were preincubated with 40 μM Z-DEVD-fmk for 1 h before the treatment of 0.5 μM EriB for 48 h. Z-DEVD-fmk completely inhibited caspase-3 activation, PARP cleavage and AML1-ETO degradation. (**c**) Kasumi-1 cells were treated as (**b**). Z-DEVD-fmk only partially decreased EriB-induced apoptosis. Each column represented the percentage of annexin V^+ cells as the mean $\pm$S.D. in triplicates in three independent experiments

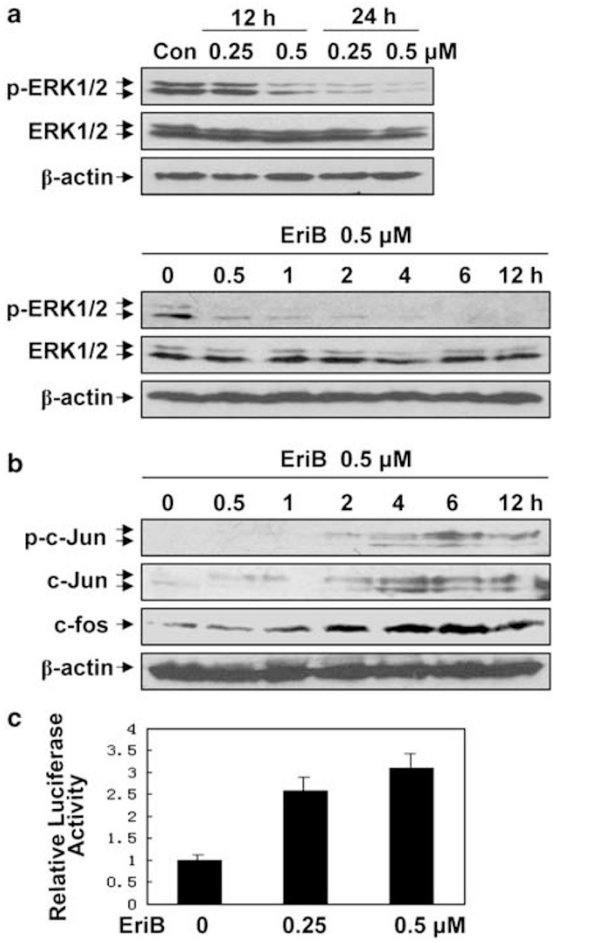

Figure 6 EriB decreased ERK phosphorylation and induced c-Jun and c-Fos expression in Kasumi-1 cells. (**a**) EriB inhibited the phosphorylation of ERK. Kasumi-1 cells were exposed to 0.25 and 0.5 μM EriB for 12 and 24 h, and Western blot analysis was performed to detect phosphorylation form of the ERK1/2 protein (upper panel). The phosphorylation of ERK1/2 was also assessed in Kasumi-1 cells after treatment with 0.5 μM EriB for 0, 0.5, 1, 2, 4, 6 and 12 h (lower panel). (**b**) EriB induced the expression of c-Jun and c-Fos. Kinetic Western blots of the phosphorylated form of c-Jun (p-c-Jun), c-Jun and c-Fos were performed in Kasumi-1 cells treated under the same condition as (**a**) (lower panel). (**c**) EriB induced an increase of AP-1-dependent transcription. Kasumi-1 cells were transiently transfected with an AP-1 directed luciferase report plasmid and a β-gal plasmid as control for transfection efficiency, and then treated with 0.25 and 0.5 μM EriB for 4 h. Each column represented the mean $\pm$S.D. in triplicates in three independent experiments

Kasumi-1 cells treated by EriB for 12 and 24 h (Figure 6a, upper panel). More precisely, this reduction of p-ERK1/2 occurred within 30 min after exposure to EriB (Figure 6a, lower panel).

Increased AP-1 activity could lead to apoptosis in human tumor cells.[18] In Kasumi-1 cells, EriB rapidly induced expression of c-Jun, c-Fos and phosphorylation form of c-Jun (Figure 6b). The c-Jun activation, as indicated by induction of its phosphorylation form, suggested its potential role on EriB-induced apoptosis. Subsequently, luciferase assay revealed that AP-1 activity was elevated approximately threefold by EriB addition for 4 h (Figure 6c), indicating that EriB increased the transcription factor activity of AP-1 probably through c-Jun activation.

EriB induced apoptosis of leukemia cells from AML patients with t(8;21) and did not affect the proliferation capacity of normal hematopoietic progenitor cells. Treatment with 0.1 and 0.25 μM EriB significantly inhibited cell growth and resulted in more than 60% cell inhibition in primary leukemia cells from all five AML patients with t(8;21), representative results from one patient are shown on Figure 7a. Typical morphological changes of apoptosis were observed (Figure 7b), accompanying with decreased Bcl-2 and Bcl-X_L levels and AML1-ETO degradation (Figure 7c). Therefore, primary t(8;21) leukemia cells responded to EriB in a similar way as Kasumi-1 cells.

However, as determined by MTT assays, proliferation of $CD34^+$ cells isolated from human cord blood, a population relatively enriched in hematipoietic progenitor cells ($n=3$), was not affected even at the concentrations up to 2.5 μM, suggesting that EriB exerted no major cytotoxic effect on normal hematopoietic precursors (Figure 7d).

***In vivo* efficacy of EriB on murine models.** C57 mice were sublethally irradiated and injected intravenously with 3×10^6 MigA/Etr cells expressing C-terminal truncated AML1-ETO (Day 0) as previously described.[19] EriB treatment (1.25 or 2.5 mg/kg, intraperitoneally daily for 2 weeks) was started on Day 5, and overall survival (OS) was measured from Day 0 to the date of death.

All the mice eventually developed symptoms of anemia (<4 g/dl hemoglobin) and labored breathing, with increased numbers of immature cells in the peripheral blood. Comparing

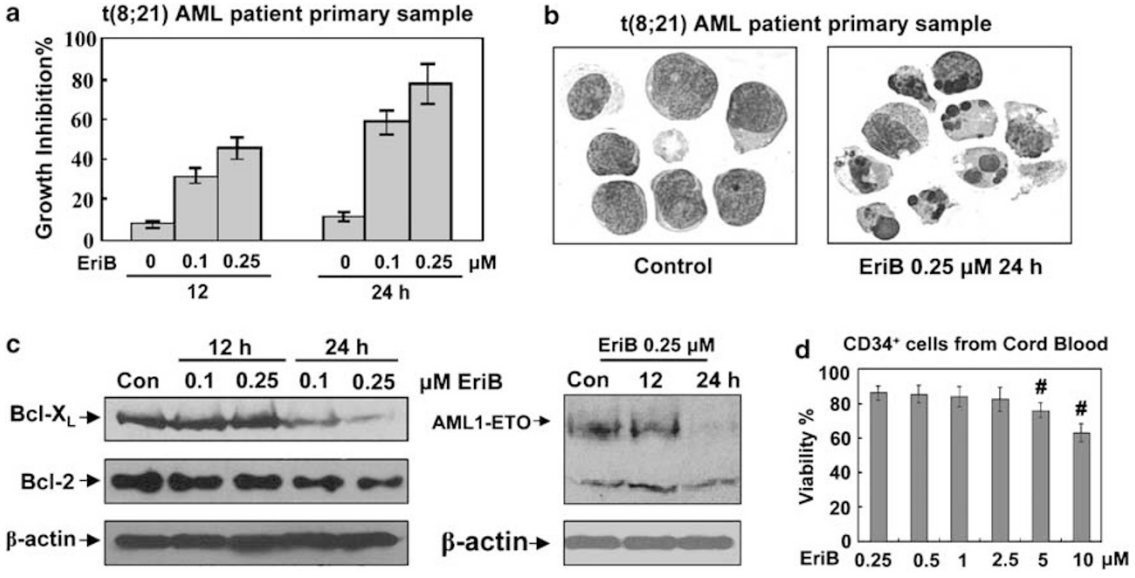

Figure 7 EriB induced apoptosis in fresh leukemic cells from AML patients with t(8;21) without affecting the proliferation capacity of normal hematopoietic progenitor cells. (**a** and **b**) EriB inhibited growth and induced apoptosis of primary leukemia cells from patients with t(8;21) leukemia. The effects were evaluated by trypan blue exclusion assay (**a**) and morphological study (**b**). (**c**) The Bcl-X_L and Bcl-2 expression were decreased in primary leukemia cells treated with 0.1 and 0.25 μM EriB for 12 and 24 h (left panel). Meanwhile, AML1-ETO protein was degraded by 0.25 μM EriB treatment. (**d**) The proliferation of normal hematopoietic progenitor cells was not inhibited by EriB up to 2.5 μM. CD34$^+$ cells enriched from cord blood samples ($n=3$) were cultured in the presence of EriB at the indicated concentrations for 72 h. The cell viability was measured by MTT assay. Each column represented the mean $\pm$ S.D. in triplicates in three independent experiments (#, $P<0.01$ *vs.* control)

with normal tissues from C57 mice, histological and morphological analysis revealed extensive infiltrations of immature blast cells in hematopoietic organs (spleen and bone marrow), which destroyed the normal architectures of these tissues (Figure 8a). In mice treated with EriB, the spleen volume was reduced (Figure 8a, lower left panel). Moreover, EriB significantly delayed disease onset in this model and showed an increase in survival time, extending the median OS from 25 to 28 (EriB 1.25 mg/kg, $P<0.001$) or 32 days (EriB 2.5 mg/kg, $P<0.001$), relative to the control group (Figure 8a, lower right panel).

Another murine model of xenograft tumor was established by subcutaneous inoculation of 3×10^7 Kasumi-1 cells (Day 0) in nude mice.[20] The latency of tumor formation at the site of injection was approximately on Day 8–12. The mice were treated with EriB (2.5 mg/kg) in the same way from Day 10 and tumor volume was measured daily until Day 19. Compared with the control group, EriB significantly reduced the tumors size ($P<0.05$) (Figure 8b).

Discussion

It has been reported that diterpenoids exert significant cytotoxicity against solid tumor cells and hematological malignant cells.[21,22] In the present study, we found that EriB, a diterpene compound isolated from *Isodon eriocalyx* var. *laxiflora*, possessed an antiproliferation effect on leukemia/lymphoma cells, especially on t(8;21) leukemia cells. This was observed not only in well-established Kasumi-1 cell line and fresh patient samples, but also in murine models of t(8;21) leukemia, suggesting that EriB may be potentially used in treating t(8;21) leukemia.

EriB decreased cell viability mainly due to the induction of apoptosis, as first demonstrated by morphological features, increment of sub-G1 cells and annexin V^+/PI^- cells. Moreover, based on the results of ultrastructural study and mitochondrial membrane potential assay, the apoptosis induced by EriB was closely related to mitochondrial pathway. Bcl-2 and Bcl-X_L, as the major antiapoptotic proteins of Bcl-2 family,[23] were significantly reduced by EriB at both mRNA and protein levels, further implying that intrinsic apoptotic pathway is involved in EriB-induced apoptosis. As previously reported, oridonin, a diterpenoid isolated from Rabdosia rubescens, could downregulate Bcl-2 expression and induce apoptosis of NB4 and K562 cells.[24] Induction of apoptosis by oridonin was also observed in T-cell leukemia MT-1 cells due to downregulated levels of Bcl-X_L.[25]

Constitutive activation of NF-κB is observed in AML and NF-κB regulates expression of many genes important for the apoptosis and survival of leukemia cells, including Bcl-2 and Bcl-X_L.[12,13,26] Various factors, including TNF-α, can activate NF-κB by degrading the NF-κB inhibitor IκBα. IκBα degradation allows NF-κB to translocate from its inactive cytoplasmic location into the nucleus and initiate the transcriptional activation of targeted genes.[27] Recently, it has been shown that oridonin treatment is associated with blockage of NF-κB signal pathways.[25,28] Directly interfering with the DNA-binding activity of NF-κB to its response DNA sequence, oridonin has an additional impact on NF-κB nuclear translocation by affecting IκBα phosphorylation and degradation.[28] In our study, we found that both mechanisms were involved in EriB-mediated inhibition of NF-κB activation. EriB inhibited the intrinsic NF-κB activation by directly interrupting the DNA-binding activity of NF-κB without the change of nuclear translocation. In the presence of TNF-α, EriB prevented

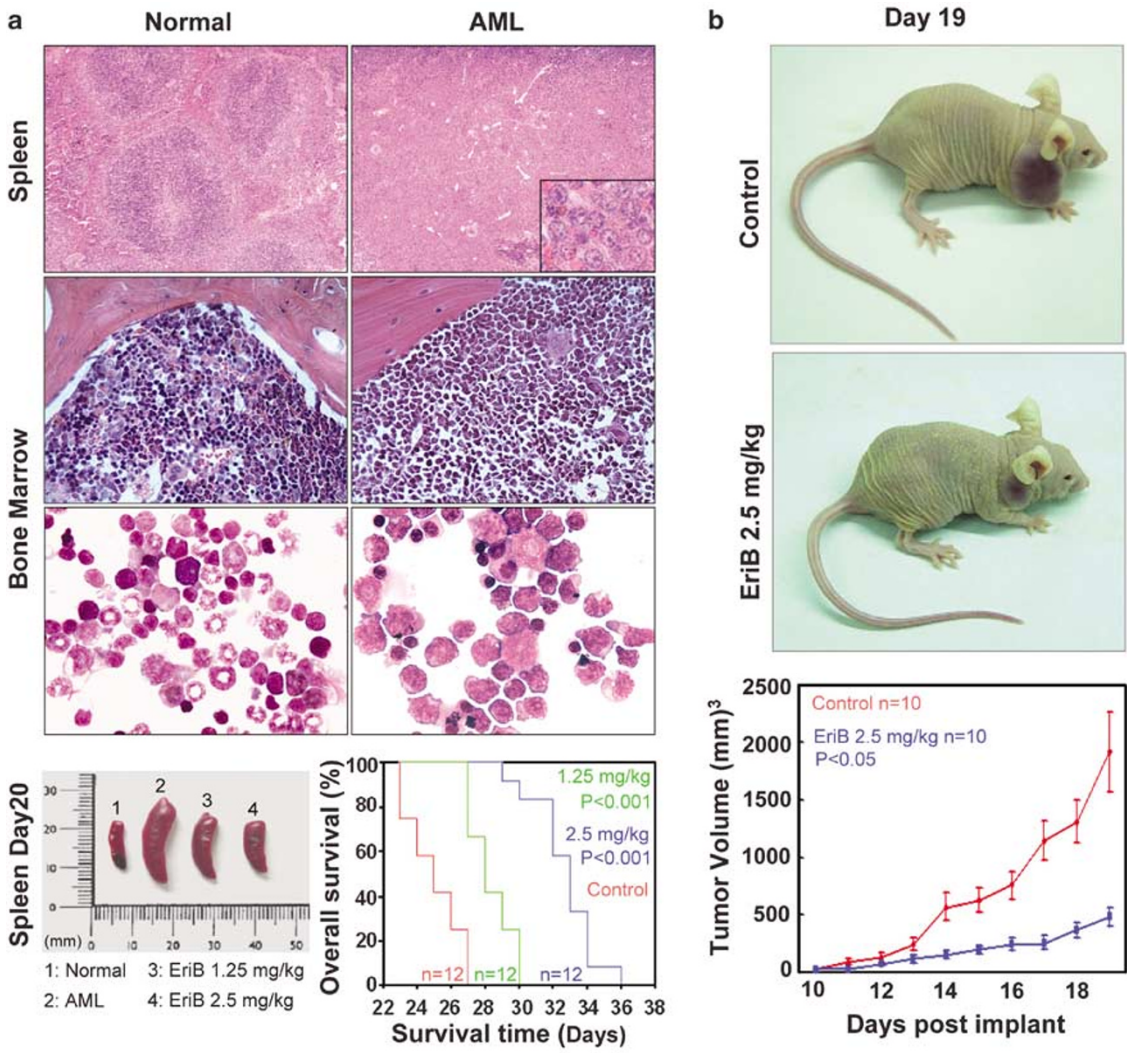

Figure 8 Effects of EriB on murine models of t(8;21) leukemia. (**a**) EriB could prolong the survival time in C57 mice model of t(8;21) leukemia. C57 mice were injected with MigA/Etr cells expressing C-terminal truncated AML1-ETO. The treatments began 5 days later including control diluent ($n=12$), 1.25 mg/kg EriB ($n=12$) and 2.5 mg/kg EriB ($n=12$) daily for 2 weeks. The mice presented leukemic involvement of spleen ($\times$ 100 and $\times$ 400, upper panel) and bone marrow ($\times$ 400 and $\times$ 1000, middle panel) comparing with normal C57 mice. EriB significantly decreased the size of spleen (Day 20) and improved overall survival time (green line: 1.25 mg/kg EriB, $P<0.001$; blue line: 2.5 mg/kg EriB, $P<0.001$), comparing with control group (red line: control, lower panel). (**b**) EriB could decrease the tumor size in nude mice model of xenograft tumor. Nude mice were injected subcutaneously with Kasumi-1 cells. The treatments began 10 days later including control diluent ($n=10$) and 2.5 mg/kg EriB ($n=10$) daily for 10 days. The tumors of control mice and EriB-treated mice on Day 19 were shown (upper and middle panel). EriB could significantly reduce the xenograft tumor volumes ($P<0.05$, lower panel). Each point represented the mean $\pm$ S.D. of 10 tumors

TNF-α-induced NF-κB activation through blocking IκBα phosphorylation and degradation. Therefore, EriB has the ability to negatively regulate NF-κB activation. Given the expression of NF-κB in AML, but not normal primitive cells, inhibition of NF-κB might induce leukemia-specific apoptosis.

Caspase-3 activation, essential for leukemia cell apoptosis, could further cleave IκBα, resulting in the loss of the ubiquitination sites and generation of a nondegradable form of IκBα (ΔIκBα). ΔIκBα acts as a super-repressor in its association with NF-κB dimmer and downregulates NF-κB activity by sequestering it in the cytosol.[14,29] EriB generated a 34-kDa cleavage product of IκBα (ΔIκBα) in a caspase-3-dependent manner, contributing to an additional decrease in nuclear NF-κB level. Apart from its role on NF-κB inhibition, it also seemed to be associated with EriB-induced degradation of AML1-ETO. This may explain why t(8;21) leukemia cells were most sensitive to EriB.

Raf/MEK/ERK cascade generally promotes cell survival, particularly in malignant hematopoietic cells.[30] AP-1 activation can provoke cell death and the main AP-1 complex members in mammalian cells are c-Jun and c-Fos.[17,31] C-Jun can act as a proapoptotic regulator in cells exposed to DNA damage via induction of Fas-L, while c-Fos has both proapoptotic and antiapoptotic functions, depending on the cell type and extracellular stimuli.[32,33] Previous study showed that oridonin could enhance L929 cell death by activating ERK-dependent MAPK pathway.[34] In this study, we demonstrated that EriB addition to Kasumi-1 cells resulted in an inhibition of ERK1/2 phosphorylation and activation of AP-1, providing evidence that EriB could interfere with ERK1/2

pathway through inactivating prosurvival signaling regulators (i.e. ERK1/2) while activating positive regulators of apoptosis (i.e. AP-1). This could represent one of the NF-κB-independent mechanisms in EriB-induced apoptosis. On the other hand, ERK1/2 could directly phosphorylate Bcl-2 on Ser-70 and this phosphorylation may be required for full and potent antiapoptotic function of Bcl-2. Based on the fact that triterpenoid CDDO-Me could inhibit ERK1/2 activation and block Bcl-2 phosphorylation, EriB may also affect this function.[35,36]

The intracellular redox status, depending on GSH levels and ROS generation, is important in keeping mitochondria stable and modulating redox-sensitive transcription factors including NF-κB during oxidative stress, since their binding abilities to target genes require a reductive environment in the nucleus.[37] When the SH groups form a disulfide bond, the redox-sensitive cysteine residues within the DNA-binding region are oxidized, making them unable to bind their target genes.[38] Having a high affinity for thiols groups, EriB changed the intracellular redox status and regulated mitochondria and NF-κB pathways through depletion of GSH and elevation of ROS. However, this working hypothesis is yet to be tested in the future.

In summary, our study demonstrated that EriB effectively induced apoptosis of t(8;21) leukemia cells through modulation of NF-κB, AML1-ETO and MAPK pathways. EriB may thus be a potential apoptosis inducer and therapeutic reagent for treatment of t(8;21) leukemia.

Materials and Methods

Reagents. EriB (provided by H-D Sun) was dissolved in DMSO as 100 mM solution and stocked at -20°C. 3-(4,5-dimethylthiazol-2-yl)-2,5-diphenyltetrazolium bromide (MTT), propidium iodide (PI), rhodamine 123 (Rh123), dichlorofluorescein diacetate (DCFH-DA), tumor necrosis factor alpha (TNF-α), dithiothreitol (DTT), protease inhibitor cocktail and Hoechst 33258 were purchased from Sigma (St Louis, MO). Z-DEVD-fmk and anti-Bcl-x antibody were purchased from BD Biosciences (San Diego, CA, USA). Anti-poly (ADP-ribose) polymerase (PARP), caspase-3, Bcl-2, Bcl-X_L, Bax, NF-κB (P65), Lamin B, carboxyl-terminal IκBα, amino-terminal IκBα, ERK1/2, phosphorylated form of ERK1/2, c-Jun, phosphorylated form of c-Jun and ETO antibodies, horseradish peroxidase-conjugated goat anti-mouse IgG, goat anti-rabbit IgG and mouse anti-goat IgG antibodies were obtained from Santa Cruz Biotechnology (Santa Cruz, CA, USA). Anti-β-actin and c-Fos antibodies were obtained from Abcam (Cambridge, UK). Anti-cleaved caspase-3, phosphorylated form of IκBα antibodies and chemiluminescence phototope-horseradish peroxidase kit were purchased from Cell Signaling (Beverly, MA, USA). Alexa Fluor 488 labeled donkey anti-rabbit IgG antibody was obtained from Molecular Probes (Eugene, OR, USA).

Cell culture, cell viability and cell morphology. The following human cell lines were used: AML leukemia with t(8;21) translocation (Kasumi-1), acute promyelocytic leukemia (NB4, NB4/R1, NB4/R2 and HL60), acute myelomonocytic leukemia (U937), chronic myelogenous leukemia (K562), Burkitt's lymphoma (Raji and Daudi) and T-cell acute lymphoblastic leukemia (Jurkat). Fresh leukemia cells were obtained from five AML patients with t(8;21), enriched by Ficoll separation. The diagnosis was established on the basis of morphological examination, presence of t(8;21) in cytogenetic study and positive RT-PCR results for AML1-ETO. Separated over Ficoll solution, $CD34^+$ cells were further isolated from human cord blood using the Direct CD34 Progenitor Cell Isolation Kit (Miltenyi Biotec Inc., Aubum, CA, USA). Informed consent was obtained according to institutional guidelines.

Leukemia cells were cultured in RPMI-1640 medium (Gibco/BRL, Grand Island, NY, USA) supplemented with 10% fetal bovine serum (HyClone Laboratories, Logan, UT, USA) in 5% CO_2-95% air humidified atmosphere at 37°C. $CD34^+$ cells were cultured as previously described.[39] Cell viability was assessed by triplicate counting of trypan blue dye-excluding cells under light microscopy. Cell morphology was evaluated by Wright's staining of cells prepared by cytospin centrifugation.

MTT reduction assay. Cells were treated with EriB at concentrations of 0.1, 0.25, 0.5, 1, 2, 4, 6, 8 and 10 μM in a 96-well plate. After 72 h, 0.1 mg MTT was added to each well. The samples were incubated at 37°C for 4 h and the absorbance was measured at 570 nm by spectrophotometry.

Flow cytometric assays for annexin-V, nuclear DNA content distribution, mitochondrial transmembrane potentials and reactive oxygen species (ROS) detection. Cell apoptosis was analyzed using an ApoAlert Annexin V-FITC Apoptosis kit (Clontech, Palo Alto, CA, USA) according to manufacturer's instructions. To assess the distribution of nuclear DNA content, cells were collected, washed in PBS and fixed overnight in 75% ethanol at -20°C, treated with 1% RNase A for at least 15 min at 37°C, and stained with 50 μg/ml PI. For mitochondrial transmembrane potential, after being washed twice with PBS, 1×10^6 cells were incubated with 10 μg/ml Rh123 for 30 min at 37°C, and stained with 50 μg/ml PI. DCFH-DA was used to measure ROS levels. Cells were washed with PBS and incubated with 20 mM DCFH-DA for 30 min at 37°C. The fluorescent intensity was measured by flow cytometry (Beckman Coulter, Miami, FL, USA).

Glutathione assessment. Glutathione (GSH) content of Kasumi-1 cells was assayed using total GSH kit (Dojin Laboratories, Kumamoto, Japan), according to manufacture's instructions.

Transmission electron microscopy. Cells were fixed in 2% glutaraldehyde at 4°C overnight and centrifuged at $3000 \times g$ for 15 min. The pellet was washed in 0.1 M cacodylate buffer, fixed in 1% buffered osmium tetroxide for 1 h at 4°C, dehydrated, and embedded in Epon 812 (TAAB Laboratories, Berkshire, UK). The sections were prepared by ultramicrotome, collected on copper grids, stained by uranyl acetate and lead citrate, and observed on electron microscopy (Philips CM120, Eindhoven, The Netherlands).

Immunofluorescence. Cells were centrifuged onto slides and fixed in methanol at -20°C for 5 min. After being washed in PBS, the slides were treated by 0.5% Triton-X, blocked with 1% BSA in PBS, incubated with anti-P65 antibody for 1 h, washed with PBS, and incubated with 488 labeled donkey anti-rabbit IgG antibody for 30 min. The slides were then incubated with Hoechst 33258 for 5 min and observed on microscopy (Olympus, Japan).

Western blot analysis. Cells (5×10^6) were harvested and lysed in 200 μl lysis buffer (0.5 M Tris-HCl, pH 6.8, 2 mM EDTA, 10% glycerol, 2% SDS and 5% β-mercaptoethanol). Protein lysates (20 μg) were electrophoresed on 10% SDS-polyacrylamide gels and transferred to nitrocellulose membranes. Membranes were blocked with 5% nonfat dried milk in TBS and incubated for 2 h at room temperature with appropriate primary antibody, followed by horseradish peroxidase-linked secondary antibody. The immunocomplexes were visualized using chemiluminescence phototope-horseradish peroxidase kit. The signal intensity of the respective bands was measured by means of the Quantity One version 4.1.1 software (Biorad, Hercules, CA, USA).

Nuclear and cytosolic fractionation. Cells (1×10^7) were incubated in 400 μl lysis buffer (10 mM HEPES (*N*-2-hydroxyethylpiperazine-*N*′-2-ethanesulfonic acid), 10 mM KCl, 1.5 mM MgCl2, 0.5 mM DTT, pH 7.9) with 0.2% Nonidet P-40 (NP-40) and protease inhibitor cocktail for 1 min on ice. After being microcentrifuged for 1 min at $2500 \times g$, the supernatants were collected as cytoplasmic protein extracts. The pellets were washed with lysis buffer without NP-40, then resuspended in 150 μl extraction buffer (20 mM HEPES, pH 7.9, 420 mM NaCl, 0.5 mM DTT, 0.2 mM EDTA and 25% glycerol), and incubated for 20 min on ice. After centrifuged at $12000 \times g$ for 10 min, the supernatants were collected as nuclear protein extracts.

Semi-quantitative reverse transcription-PCR (RT-PCR). Total RNA was extracted using Trizol and reverse transcribed into cDNA with random hexamers using Superscript II (Invitrogen) according to the manufacture's instructions. The primers used in this study were: GAPDH, 5′-TCACCAGGGCTGCTTTTA-3′ and 5′-AAGGTCATCCCTGAGCTGAA-3′, Bcl-2, 5′-GCAGGCATGTTGACTTCACTT-3′ and 5′-GGAGGATTGTGGCCTTCTTTG-3′,

Bcl-XL, 5′-CATGGCAGCAGTAAAGCAAGC-3′ and 5′-TGCGATCCGACTCACCA ATAC-3′ and Bax, 5′-TTCTGACGGCAACTTCAACTGGG-3′ and 5′-TTCT TCCAGATGGTGAGCGAGG 3′. Cycle parameters were: 94°C 5 min; 28 cycles of 94°C 1 min, 58°C 1 min, 72°C 1 min; 72°C 10 min.

Bcl-2 and Bcl-X_L transfection in Kasumi-1 cells. Kasumi-1 cells, incubated with pSFFV/Bcl-2 (PS.Bcl-2) or pSFFV/Bcl-X_L (PS.Bcl-X_L) or a control expression vector pSSFV, were electroporated at 1000 V 25 microfarads in 4-mm cuvettes using a Bio-Rad Gene Pulser (Hercules, CA, USA) and replated in fresh medium.

Luciferase assay. Kasumi-1 cells were incubated with a report gene construct (10 μg of NF-κB-directed luciferase report plasmid or pAP1-luc (Clontech, Palo Alto, CA, USA)) in combination with a CMV-driven β-galactosidase expression plasmid (2 μg) to assess transfection efficiency, and were electroporated as described above. After 36 h of transfection, cells were exposed to EriB and/or TNFα, and lysed with passive lysis buffer (Promega, Madison, WI, USA). Luciferase activities were measured with lumat LB 9507 tube luminometer (EG&G Berthold, Bundoora, Australia). To measure β-galactosidase activity, cell lysates were mixed with 2 $\times$ β-galactosidase assay reagent (1.33 mg/ml *o*-nitrophenyl-β-D-galactopyranoside, 120 mM Na_2HPO_4, 80 mM NaH_2PO_4, 2 mM $MgCl_2$ and 100 mM β-mercaptoethanol, pH 7.4) in a total volume of 300 μl. The mixture was incubated at 37°C for 1 to 6 h and quenched by adding 700 μl of 1 M Na_2CO_3. The β-galactosidase activity was measured at 420 nm by spectrophotometry.

Electrophoretic mobility shift assays (EMSA). Nuclear extracts of Kasumi-1 cells were prepared and protein content was determined using Coomassie Plus reagent (Pierce, Rockford, IL, USA). Nuclear extracts (10 μg) were incubated with ^{32}P-end-labeled double-stranded NF-κB consensus oligonucleotide (5′-AGTTGAGGGGACTTTCCCAGGC-3′) (Promega, Madison, WI, USA). The incubation mixtures were separated by 4% nondenaturing PAGE and the bands were detected by autoradiography.

Murine model of t(8;21) leukemia. Female C57 mice and nude mice (5–6 weeks of age) were bred and maintained in pathogen-free conditions. C57 mice received 400 cGy from a high-energy linear accelerator (6MV, SIEMENSPRIMUS) at the dose-rate of 100 cGy/min. After 24 h, the C57 mice were injected with 3 $\times$ 10^6 MigA/Etr cells expressing C-terminal truncated AML1-ETO in 0.2 ml PBS via tail vein. Treatments (12 mice per group) were started 5 days after leukemic cells injections. The control group and the EriB group received, respectively, EriB (1.25 or 2.5 mg/kg, intraperitoneally for 2 weeks) and control diluent (1% Pluronic F68 in deionized water).

In nude mice *(nu/nu)*, Kasumi-1 cells (3 $\times$ 10^7) were injected subcutaneously into the right flank. Treatments (10 mice per group) were started on 10 days after leukemic cells injections. EriB (2.5 mg/kg) and control diluent were administered intraperitoneally for 10 days. Tumor volumes were calculated by the formula: $0.5 \times a \times b^2$ in millimeters, where '*a*' is the length and '*b*' is the width. Tissue samples were fixed in formaldehyde and further processed for paraffin embedding.

Statistical analysis. All the results were expressed as the mean $\pm$ S.D. of data obtained from three separate experiments and determined using *t*-test to compare variance. Survival functions were estimated using the Kaplan–Meier method and compared by the log-rank test. *P*-values <0.05 were considered statistically significant. All statistical analyses were evaluated using SAS 8.2 software (SAS Institute Inc, Cary, NC, USA).

Acknowledgements. The authors thank Dr. Dong-Er Zhang (The Scripps Institute, La Jolla, CA, USA) for providing MigA/Etr cells and Dr. Paul B Fisher (Columbia University, NY, USA) for providing plasmid pSFFV/Bcl-2, pSFFV/Bcl-X_L and pSSFV. We thank Dr. Yu-Hong Xu and Xiao-Hui Wei (Shanghai Jiao Tong University), Ting-Jun Ye, Ping Zhu, Zu-Guang Xia and Yuan-Hua Liu for technical assistance and Zhao-Jun Wen for illustrations.

This work was supported, in part, by the Chinese National Key Program for Basic Research (973:2004CB518600), the Chinese National High Tech Program (863:2002BA711A04), the National Natural Science Foundation of China (90209007 and 30400590), the Key Discipline Program of Shanghai Municipal Education Commission (Y0201), the Shanghai Commission of Science and Technology (04DZ14004 and 44107025), the Shanghai Rising Star Program (05QMX1429), the Natural Science Foundation of Yunnan Province (2004C008Z), and by the Samuel Waxman Cancer Research Foundation Laboratory.

1. McCulloch EA. Stem cells in normal and leukemic hemopoiesis. *Blood* 1983; **62**: 1–13.
2. Look AT. Oncogenic transcription factors in the human acute leukemias. *Science* 1997; **278**: 1059–1064.
3. Peterson LF, Zhang DE. The 8;21 translocation in leukemogenesis. *Oncogene* 2004; **23**: 4255–4262.
4. Wang YY, Zhou GB, Yin T, Chen B, Shi JY, Liang WX *et al.* AML1-ETO and C-KIT mutation/overexpression in t(8;21) leukemia: implication in stepwise leukemogenesis and response to Gleevec. *Proc Natl Acad Sci USA* 2005; **102**: 1104–1109.
5. Hamblin TJ. Disappointments in treating acute leukemia in the elderly. *N Engl J Med* 1995; **332**: 1712–1713.
6. Mann J. Natural products in cancer chemotherapy: past, present and future. *Nat Rev Cancer* 2002; **2**: 143–148.
7. Shen ZX, Chen GQ, Ni JH, Li XS, Xiong SM, Qiu QY *et al.* Use of arsenic trioxide (As2O3) in the treatment of acute promyelocytic leukemia (APL), II. Clinical efficacy and pharmacokinetics in relapse patients. *Blood* 1997; **89**: 3354–3360.
8. Ikezoe T, Chen SS, Tong XJ, Heber D, Taguchi H, Koeffler HP. Oridonin induces growth inhibition and apoptosis of a variety of human cancer cells. *Int J Oncol* 2003; **23**: 1187–1193.
9. Sun HD, Xu YL, Jiang B. *Diterpenoids from Isodon Species*. Beijing: Science Press, 2001 pp. 95–104.
10. Kroemer G, Reed JC. Mitochondrial control of cell death. *Nat Med* 2000; **6**: 513–519.
11. Cory S, Adams JM. The Bcl2 family: regulators of the cellular life-or-death switch. *Nat Rev Cancer* 2002; **2**: 647–656.
12. Catz SD, Johnson JL. Transcriptional regulation of bcl-2 by nuclear factor kappa B and its significance in prostate cancer. *Oncogene* 2001; **20**: 7342–7351.
13. Pahl HL. Activators and target genes of Rel/NF-kappaB transcription factors. *Oncogene* 1999; **18**: 6853–6866.
14. Reuther JY, Baldwin Jr AS. Apoptosis promotes a caspase-induced amino-terminal truncation ofIkappaBalpha that functions as a stable inhibitor of NF-kappaB. *J Biol Chem* 1999; **274**: 20664–20670.
15. Steffen B, Serve H, Berdel WE, Agrawal S, Linggi B, Buchner T *et al.* Specific protein redirection as a transcriptional therapy approach for t(8;21) leukemia. *Proc Natl Acad Sci USA* 2003; **100**: 8448–8453.
16. Fischer U, Schulze-Osthoff K. Apoptosis-based therapies and drug targets. *Cell Death Differ* 2005; **12** (Suppl 1): 942–961.
17. Milella M, Kornblau SM, Estrov Z, Carter BZ, Lapillonne H, Harris D *et al.* Therapeutic targeting of the MEK/MAPK signal transduction module in acute myeloid leukemia. *J Clin Invest* 2001; **108**: 851–859.
18. Eferl R, Wagner EF. AP-1: a double-edged sword in tumorigenesis. *Nat Rev Cancer* 2003; **3**: 859–868.
19. Yan M, Burel SA, Peterson LF, Kanbe E, Iwasaki H, Boyapati A *et al.* Deletion of an AML1-ETO C-terminal NcoR/SMRT-interacting region strongly induces leukemia development. *Proc Natl Acad Sci USA* 2004; **101**: 17186–17191.
20. Hao CL, Lin D, Wang LH, Xing HY, Wang M, Wang JX. Combination of phenylbutyrate and 5-Aza-2'deoxycytidine inhibits human Kasumi-1 xenograft tumor growth in nude mice. *Zhonghua Xue Ye Xue Za Zhi* 2004; **25**: 658–661.
21. Chen S, Gao J, Halicka HD, Huang X, Traganos F, Darzynkiewicz Z. The cytostatic and cytotoxic effects of oridonin (Rubescenin), a diterpenoid from Rabdosia rubescens, on tumor cells of different lineage. *Int J Oncol* 2005; **26**: 579–588.
22. Liu JJ, Wu XY, Peng J, Pan XL, Lu HL. Antiproliferation effects of oridonin on HL-60 cells. *Ann Hematol* 2004; **83**: 691–695.
23. Kroemer G. The proto-oncogene Bcl-2 and its role in regulating apoptosis. *Nat Med* 1997; **3**: 614–620.
24. Liu J, Huang R, Lin D, Wu X, Peng J, Lin Q *et al.* Apoptotic effect of oridonin on NB4 cells and its mechanism. *Leuk Lymphoma* 2005; **46**: 593–597.
25. Ikezoe T, Yang Y, Bandobashi K, Saito T, Takemoto S, Machida H *et al.* Oridonin, a diterpenoid purified from Rabdosia rubescens, inhibits the proliferation of cells from lymphoid malignancies in association with blockade of the NF-kappa B signal pathways. *Mol Cancer Ther* 2005; **4**: 578–586.
26. Guzman ML, Neering SJ, Upchurch D, Grimes B, Howard DS, Rizzieri DA *et al.* Nuclear factor-kappaB is constitutively activated in primitive human acute myelogenous leukemia cells. *Blood* 2001; **98**: 2301–2307.
27. Meyer R, Hatada EN, Holumann HP, Haiker M, Bartsch C, Rothlisberger U *et al.* Cloning of the DNA-binding subunit of human nuclear factor kappa B: the level of its mRNA is strongly regulated by phorbol ester or tumor necrosis factor alpha. *Proc Natl Acad Sci USA* 1991; **88**: 966–970.
28. Leung CH, Grill SP, Lam W, Han QB, Sun HD, Cheng YC. Novel mechanism of inhibition of nuclear factor-kappa B DNA-binding activity by diterpenoids isolated from *Isodon rubescens*. *Mol Pharmacol* 2005; **68**: 286–297.
29. Barkett M, Xue D, Horvitz HR, Gilmore TD. Phosphorylation of IkappaB-alpha inhibits its cleavage by caspase CPP32 in vitro. *J Biol Chem* 1997; **272**: 29419–29422.
30. Dai Y, Rahmani M, Pei XY, Khanna P, Han SI, Mitchell C *et al.* Farnesyltransferase inhibitors interact synergistically with the Chk1 inhibitor UCN-01 to induce apoptosis in

human leukemia cells through interruption of both Akt and MEK/ERK pathways and activation of SEK1/JNK. *Blood* 2005; **105**: 1706–1716.
31. van den Brink MR, Kapeller R, Pratt JC, Chang JH, Burakoff SJ. The extracellular signal-regulated kinase pathway is required for activation-induced cell death of T cells. *J Biol Chem* 1999; **274**: 11178–11185.
32. Verheij M, Bose R, Lin XH, Yao B, Jarvis WD, Grant S *et al.* Requirement for ceramide-initiated SAPK/JNK signalling in stress-induced apoptosis. *Nature* 1996; **380**: 75–79.
33. Kolbus A, Herr I, Schreiber M, Debatin KM, Wagner EF, Angel P. c-Jun-dependent CD95-L expression is a rate-limiting step in the induction of apoptosis by alkylating agents. *Mol Cell Biol* 2000; **20**: 575–582.
34. Zhang CL, Wu LJ, Tashiro S, Onodera S, Ikejima T. Oridonin induces a caspase-independent but mitochondria- and MAPK-dependent cell death in the murine fibrosarcoma cell line L929. *Biol Pharm Bull* 2004; **27**: 1527–1531.
35. Deng X, Ruvolo P, Carr B, May Jr WS. Survival function of ERK1/2 as IL-3-activated, staurosporine-resistant Bcl2 kinases. *Proc Natl Acad Sci USA* 2000; **97**: 1578–1583.
36. Konopleva M, Tsao T, Ruvolo P, Stiouf I, Estrov Z, Leysath CE *et al.* Novel triterpenoid CDDO-Me is a potent inducer of apoptosis and differentiation in acute myelogenous leukemia. *Blood* 2002; **99**: 326–335.
37. Friesen C, Kiess Y, Debatin KM. A critical role of glutathione in determining apoptosis sensitivity and resistance in leukemia cells. *Cell Death Differ* 2004; **11** (Suppl 1): S73–S85.
38. Haddad JJ. Antioxidant and prooxidant mechanisms in the regulation of redox(y)-sensitive transcription factors. *Cell Signal* 2002; **14**: 879–897.
39. Yin T, Wu YL, Sun HP, Sun GL, Du YZ, Wang KK *et al.* Combined effects of As4S4 and imatinib on chronic myeloid leukemia cells and BCR-ABL oncoprotein. *Blood* 2004; **104**: 4219–4225.